3-D FRONT RECONSTRUCTION FROM RADARSAT-1 SAR DATA

Maged Marghany and Mazlan Hashim
Department of Remote Sensing
Faculty of Geoinformation Science and Engineering
Universiti Teknologi Malaysia
81310 UTM, Skudai, Johore Bahru, Malaysia
Emails: maged@fksg.utm.my,mazlan@fksg.utm.my

KEYWORDS: front, RADARSAT-1 SAR, Velocity bunching, Volterra, B-spline, 3-D.

ABSTRACT

This paper presents work done to utilize RADARSAT-1 SAR data to reconstruct 3-D of coastal water front. The velocity bunching model used to extract the significant wave height from RADARSAT-1 SAR while the Volttera model used to model the front movements. B-spline also is implemented to reconstruct the front into 3-D. This study shows that the integration between velocity bunching, Volttera models and B-spline can be used as geomatica tool for 3-D front reconstruction.

1. INTRODUCTION

Fronts play a role of tremendous importance in oceanography dynamics in several ways. Dynamically, they are of considerable importance of understanding turbulent energy cascade from ocean surface down to billow-turbulence scales of a few meters (Robinson 1995). Coastal pollutant material transports are directed by turbulent energy flow vertically through water body. In addition, productivity of ocean can be enhanced due to fronts since they tend to bring nutrient rich water. Scientists reported that fish stocks increased as results of combination of warm water and nutrients arising from cross-frontal mixing. Furthermore, fronts also have a great deal to insure search and rescue operations, since a

drifting stricken small craft will remain in a front even when exposed to considerable wind, particularly when it is partly filled with water and nearly completely submerged(Simpson and Pingree 1978). Even though, traditional methods for front studies are depended on in-situ measurements of sea water temperature and salinity they might be costly and time consuming. Isothermal, isohaline contours and water mass diagrams are classical procedures for front detection nevertheless front cannot be visualized in large scale surface ocean (Simpson 1981)

According to above mentioned, remote sensing techniques are able to image front locations in large scale ocean. Both thermal and microwave remote sensing techniques are good tools to identify front locations. For instance, satellite infrared imagery can image front locations due to their strong thermal signatures. Moreover, satellite visible bands are also cable to image fronts based on imaging different colors of the two water masses. Besides that, synthetic aperture radar (SAR) are also able to identify front due to abruptly changes of surface wave pattern across front led to greatly change cross backscatter of SAR data.
In this paper, we emphasize how 3-D front can be reconstructed from single SAR data (namely the RADARSAT-1 SAR) using integration of Volterra kernel (Ingland and Garello, 1990), velocity bunching and Fuzzy B-spline models (Maged et al., 2002). There are approximately three hypothesis that examined are: (i) The use of Volterra model to detect front flow pattern from RADARSAT-1 SAR C_{HH} band; (ii) the use of velocity bunching model to obtain significant wave height from RADARSAT-1 SAR data; and (iii) the utilization of Fuzzy B-spline to reconstruct 3-D of front surface.

2. METHODOLOGY

2.1 Data Set and In-situ Measurement

The RADARSAT-1 SAR fine mode data were acquired on March 26, 2004 over the coastline of Kuala Terengganu, Malaysia (103^0 5'E to 103^0 9'E and 5^0 20 N to 5^0 27' N). The RADARSAT-1 SAR fine mode data are acquiring information using C band HH polarized of frequency 5.3GHz. The swath width of RADARSAT-1 SAR fine mode sensor is 50km, with range resolution of 8-9km. There are two numbers of looks for The RADARSAT-1 SAR and the incident angle of 35^0-49^0.

Ocean wave spectra parameters such as wavelength, direction and significant wave height are collected using AWAC wave rider buoy during satellite pass over. AWAC wave rider buoy is deployed by 6 hours before and satellite Passover.

2.2 3-D Front Model

There are three models involved for 3-D front reconstruction; velocity bunching, Volterra and Fuzzy B-spline. Significant wave heights are simulated from RADARSAT-1 SAR image by using velocity bunching model. Fuzzy B-spline used significant wave height information to reconstruct 3-D front. Moreover, front flow pattern is modeled by Volterra model (Figure 1).

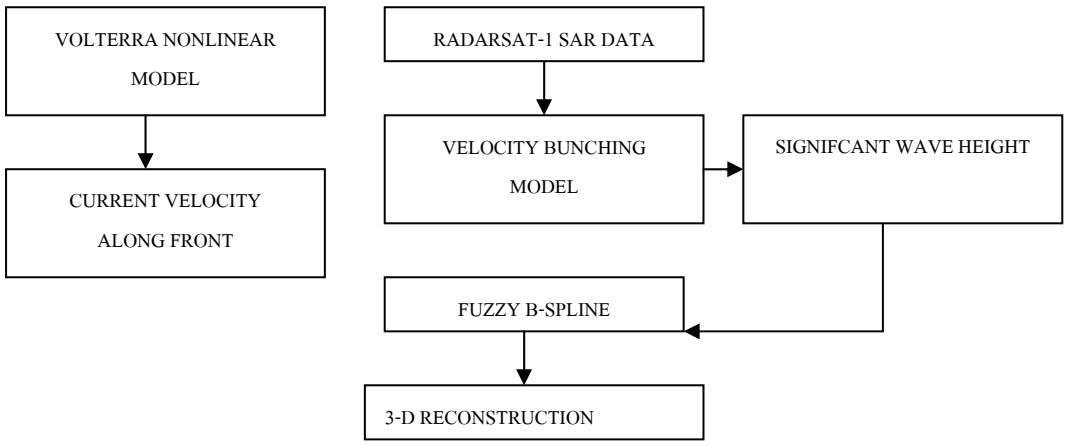

Figure 1 Block Diagram for RADARSAT-1 SAR data Processing

2.3 Velocity Bunching Model

In this study, two dimension Fourier Transform (2-DFFT) has been applied to a single SAR image frame comprising of 512 x 512 image pixels which was extracted from RADARSAT-1SAR image. The Gaussian algorithm was applied to remove the noise from the image and smoothen the wave spectra into normal distribution curve. The band used in this processing was C_{HH}-band. Each pixel represents a 12.5 m x 12.5 m area for RADARSAT-1SAR image. The entire image frame of RADARSAT-1SAR image corresponds to a 6.4 km x 6.4 km patch on the ocean surface. This frame size provides a sufficiently large area to include at least 10 cycles of very long surface waves, up to 640 m in length, which can be

included in a single image frame. It is also small enough to show that the ocean can be reasonably assumed homogeneous within a frame (Maged 2004).

The velocity bunching MTF is the dominant component of the linear MTF for the ocean waves with an azimuth wave number (k_x). According to Alpers *et al*., (1981); Vachon *et al*., (1993, 1994, 1995 and 1997), the velocity bunching can contribute to linear MTF based on the following equation

$$M_v = \frac{R}{V}\omega\left[\frac{k_x}{k}\sin\theta + i\cos\theta\right] \tag{1}$$

where R/V is the scene range to platform velocity ratio, which is 111 s in the case of RADARSAT-1SAR image data, θ is RADARSAT-1SAR image incidence angel (35^0-49^0) and ω is wave spectra frequency which equals to $2\prod$/K. To estimate the velocity bunching spectra $S_{vb}(k)$, we modified the algorithm that was introduced by Krogstad and Schyberg (1991). The modification is to multiply the velocity bunching MTF (M_v) by RADARSAT-1SAR image spectra variance of the azimuth shifts. This can be calculated by using the following formula:

$$S_{vb}(k) = [I_0 \sum_{n=1}^{\infty} \frac{\psi(k_x)^{2n}}{n!} S_{\zeta\zeta}{}^{*n} \psi(k)^2 e^{-K_x{}^2 \rho_{\zeta\zeta}}][M_v] \tag{2}$$

where $S_{\zeta\zeta}$ is the SAR spectra variance of the azimuth shifts due to the surface motion, which was induced by the velocity bunching effect in azimuth direction due to high value of R/V. Furthermore, SAR spectra of ocean wave images have a characteristic of azimuth cutoff and also have an intrinsic azimuth cutoff that in many cases fit very well with actual observation and relates to the cutoff directly to the standard deviation of the azimuth shift , which may be compactly related to fundamental sea state parameters. $\rho_{\zeta\zeta}$ is the variance of the derivative of displacements along the azimuth direction, I_0 is SAR image intensity and "*n" means (n-1) –fold convolution according to Krogsted and Schyberg (1991). Equation 2 Is used to draw the velocity bunching spectra energy contours.

Estimation of Significant Wave Height from Velocity Bunching Spectra based on the azimuth cut-off arising from the velocity-bunching model, equation (2), the azimuth cutoff could be scaled by the standard deviation of the azimuth shift. Vachon et al.,(1993) introduced a relationship between the variance of the derivate of displacement along the azimuth direction $\rho_{\zeta\zeta}$ and the standard deviation of the azimuth shift σ which were estimated from the velocity bunching spectra. This relationship was given by

$$\sigma = \sqrt{\rho_{\zeta\zeta}} \qquad \text{Vachon et al., (1993)} \qquad (3)$$

The relation between standard deviation of the azimuth shift σ and significant wave height H_s can be given by

$$\sigma = (\frac{R}{V})(1 - \frac{\sin^2(\theta)}{2})^{0.5}(\frac{k_x g}{8})^{0.5} H_s \qquad \text{(Vachon et al., 1994)} \qquad (4)$$

where k_x is the azimuth wave number, θ is RADARSAT-1SAR image incident angle, *R/V* is the scene range to platform velocity ratio and g is the acceleration due to the gravity. Note that the mean wave period T_0 is equal to $2\pi(\langle\langle k_x \rangle g)^{-0.5}$. Using equation 6 and equation 4, the significant wave height H_s can be obtained:

$$H_s = 0.6(\rho_{\zeta\zeta})^{0.5}[\frac{1+\theta^2/4}{R/V}]T_0 \qquad (5)$$

where θ is the RADARSAT-1SAR incidence angle and equation 5 Is used to estimate the significant wave height which is based on the standard deviation of the azimuth shift σ.

2.4 Volterra Model

In refereeing to Ingland and Garello, (1990), Volterra series can be used to model nonlinear imaging mechanisms of surface current gradients by RADARSAT-1 SAR image. As result of that Volterra linear kernel is contained most of RADARSAT-1 SAR energy which used to simulate current flow along range direction. Following Ingland and Garello, (1990) Volterra kernel filter has the following expression:

$$H_{1y}(v_x, v_y) = k_y \vec{U}.\frac{\partial x}{\partial u_x}\left[\vec{K}^{-1}[\frac{\partial}{\partial t} + \frac{\partial \vec{c}_g}{\partial x} + \frac{\partial \vec{u}_x}{\partial x} + 0.043\frac{(\vec{u}_a\vec{K})^2}{\omega_0}\right].\left[\frac{\partial \psi}{\partial \omega}\right].$$
$$\frac{\vec{c}_g(\vec{K})\vec{U} + j.0.043(\vec{u}_a\vec{K})^2\omega_0^{-1}}{[\vec{c}_g(\vec{K})\vec{U}]^2 + [0.043(\vec{u}_a\vec{K})^2\omega_0^{-1}]^2} + j.(0.6.10^{-2}.\vec{K}^{-4})(\frac{R}{V})\vec{u}_x \quad (6)$$

where $\vec{U}$ is the mean current velocity, $\vec{u}_x$ is the current flow while $\vec{u}_a$ is current gradient along azimuth direction, respectively. k_y is the wave number along range direction, $\vec{K}$ is the spectra wave number, ω_0 is the angular wave frequency, $\vec{c}_g$ is the wave velocity group, ψ is the wave spectra energy and *R/V* is the range to platform velocity ratio.

In reference to Ingland and Garello, (1990), the inverse filter $G(v_x, v_y)$ is used since $H_{1y}(v_x, v_y)$ has a zero for (v_x, v_y) which indicates the mean current velocity should have a constant offset. The inverse filter $G(v_x, v_y)$ can be given as

$$G(v_x, v_y) = \begin{cases} [H_{1y}(v_x, v_y)]^{-1} & \text{If } (v_x, v_y) \neq 0, \\ 0 & \textit{otherwise.} \end{cases} \quad (7)$$

Using equation 6 into 7, range current velocity $U_y(0, y)$ can be estimated by

$$U_y(0, y) = I_{RADARSAT-1SAR}.G(v_x, v_y) \quad (8)$$

where $I_{RADARSAT-1SAR}$ is the frequency domain of Radarsat-1 SAR image acquired by applying 2-D Fourier transform on RADARSAT-1 SAR image.

2.5 The Fuzzy B-splines Method

Based on significant wave height modeled by using velocity bunching and radar backscatter cross section across front, Fuzzy numbers are generated. In doing so,two basic notions that we combined together: confidence interval and presumption level. A confidence interval is a real values interval which provides the sharpest enclosing range for significant wave height values. An assumption level μ -level is an estimated truth value in the [0,1] interval on our knowledge level of gradient change of significant wave heights (Anile 1997). The 0 value corresponds to minimum knowledge of significant wave heights, and 1 to the maximum of significant wave height. A fuzzy number is then prearranged in the confidence interval set,

each one related to a assumption level $\mu \in$ [0,1]. Moreover, the following must hold for each pair of confidence interval which define a number: $\mu \succ \mu' \Rightarrow h \succ h'$. Let us consider a function $f : h \to h$, of N fuzzy variables $h_1, h_2, ..., h_n$. Where h_n are the global minimum and maximum values of significant wave heights The construction begins with the same pre-processing aimed at the reduction of measured significant wave height values into a uniformly spaced grid of cells. Then, a membership function is defined for each pixel element which incorporates the degrees of certainty of radar cross backscatter.

3. RESULTS AND DISCUSSION

Figure 2 shows the signature of current boundary which can turn up as a result of brightness frontal curved line. Furthermore, it is clear that the front occurred close to estuary, which is a clear indications of tidal front events. In fact, the interaction of flood tidal current flow from estuary with topography can form a tidal front.

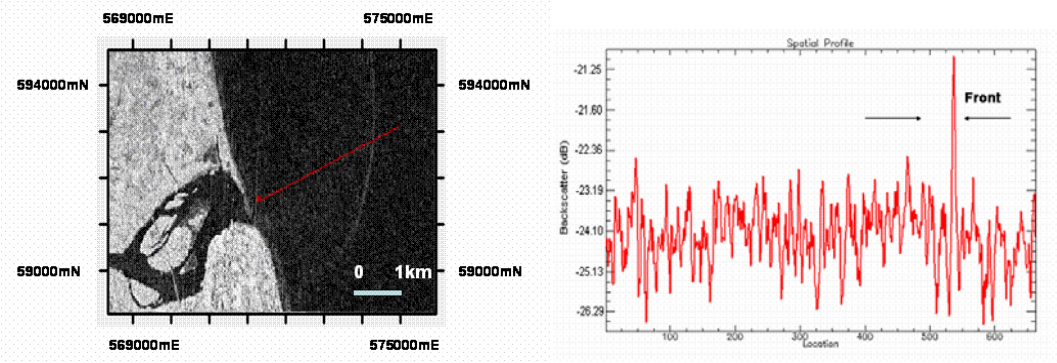

Figure 2 Front signature in RADARSAT-1 SAR and its Backscatter Values

The RADARSAT-1 backscatter cross-section across front has a maximum value of -21.25dB. It is known the maximum backscatter values of 0.33 dB is found across the brightness frontal line. Moreover, the variation of radar backscatter cross-section is due to current boundary gradient. According to Vogelzang et al.,(1997), ocean current boundaries are often accompanied by the changes in the surface roughness that can be detected by SAR. These surface roughness changes are due to the interaction of surface waves directly with surface current gradients. These interactions can cause an increase in the surface roughness and radar backscatter (Shuchman and LyzengaL 1985). Figure 3 shows 3-D front reconstruction with significant wave heights and current variations cross front. Figure 3

shows that significant wave variation cross front with maximum significant wave height of 1.2 m and gradient current of 0.9 m/s. In fact March represents the northeast monsoon period as coastal water currents in the South China Sea tend to move from the north direction (Maged 1994). Furthermore, Maged (1994) quoted that strong tidal current is a dominant feature in the South China Sea with maximum velocity of 1.5 m/s. The visualization of 3-D front is sharp with the RADARSAT-1 SAR C_{HH} band due to the fact that each operations on a fuzzy number becomes a sequence of corresponding operations on the respective μ and μ'-levels, and the multiple occurrences of the same fuzzy parameters evaluated as a result of the function on fuzzy variables (Anile 1997). Typically, in computer graphics, two objective quality definitions for Fuzzy B-splines were used: triangle-based criteria and edge-based criteria. Triangle-based criteria follow the rule of maximization or minimization, respectively, the angles of each triangle. The so-called max-min angle criterion prefers short triangles with obtuse angles.

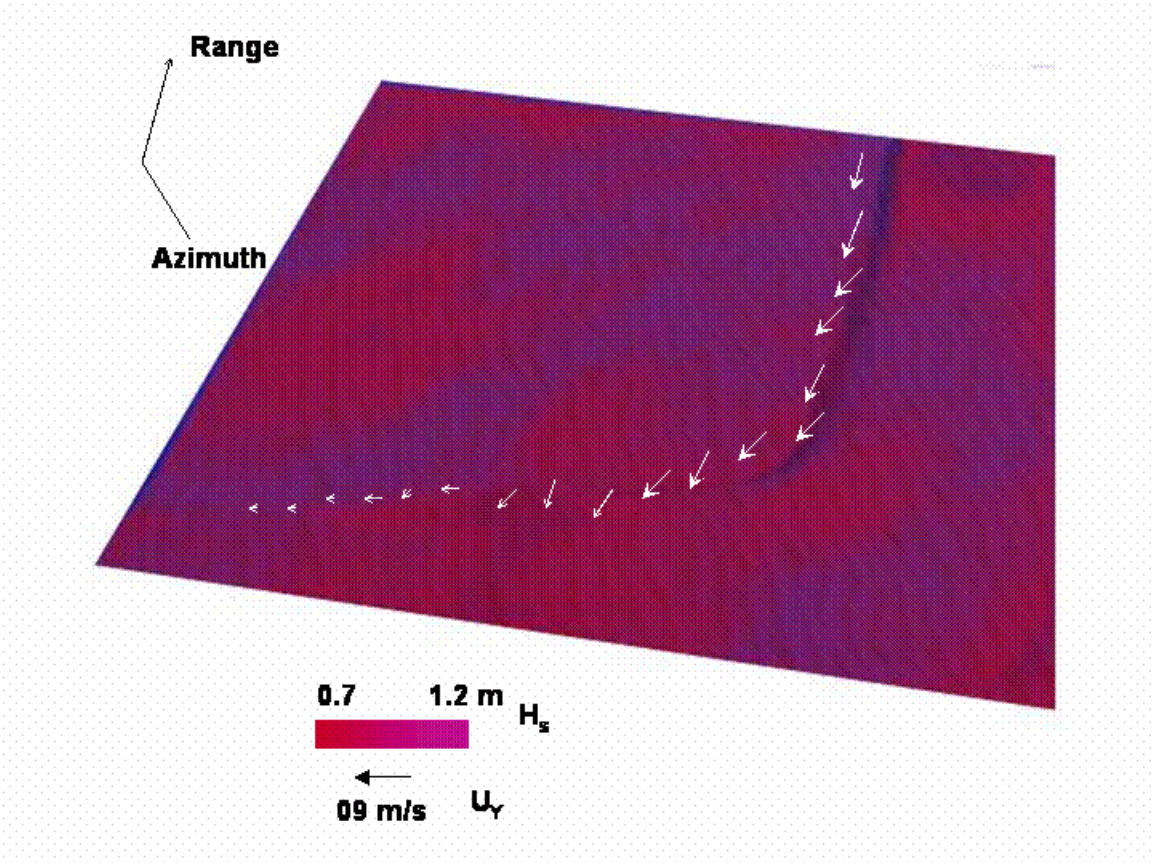

Figure 3 3-D Front Reconstruction with Significant Wave Height (Hs) and Surface Current Variations (Uy)

4. CONCLOUSION

This paper demonstrated work done to utilize Fuzzy B-spline to reconstruct ocean surface features such as front by RADARSAT-1 SAR data. Velocity bunching model extracted the elevation of ocean surface which important in building up the topology information requested in Fuzzy B-spline. Front is generated due to tidal current interaction between estuary and ocean. Front is characteristics by 0.9 m/s current flow which concaved along coastal water. In conclusion, Fuzzy B-spline model is considered as good tool to visualize ocean surface feature such as front.

REFERENCES

Alpers, W.R., Ross, D.B. and C.L. Rufenach (1981). On the detectability of ocean surface waves by real and synthetic aperture radar. J. Geophysical Research, 86:6481-6498.

Anile, A. M, (1997) *Report on the activity of the fuzzy soft computing group*, Technical Report of the Dept. of Mathematics, University of Catania, March 1997, pages 10.

Anile, AM, Deodato, S, Privitera, G, (1995) *Implementing fuzzy arithmetic*, Fuzzy Sets and Systems, 72.

Inglada, J. and Garello R.,(1999) Depth estimation and 3D topography reconstruction from SAR images showing underwater bottom topography signatures. In *Proceedings of IGARSS'99.*

Krogstad, H.E., and Schyberg, H. (1991). On Hasselman 's nonlinear ocean –SAR transformation, *Proc. of IGARSS'91*, held at Espo, Finland from Jun. 3-6, 1991, pp:841-849.

Maged M, (1994). Coastal Water Circulation off Kuala Terengganu, Malaysia". MSc. Thesis Universiti Pertanian Malaysia.

Maged M. (2004) velocity Bunching Model for Modelling wave Spectra Along east Coast of Malaysia. J. Indian Scocity of Remote Sensing. Vol (32) (2). pp:185-198.

Maged M., H. L. Mohd., and K., Yunus. (2002), TOPSAR Model for bathymetry Pattern Detection along coastal waters of Kuala Terengganu, Malaysia. Journal of Physical Sciences. Vol (14)(3), 487-490.

Robinson, I.S. (1994) Satellite Oceanography: An Introduction for Oceanographers and Remote –sensing Scientists. Johan Wiley &Sons. New York.

Shuchman, R.A., Lyzenga, D.R. and Meadows, G.A. (1985)., Synthetic aperture radar imaging of ocean-bottom topography via tidal-current interactions: theory and observations, *Int. J. Rem. Sens.*, **6**, 1179-1200.

Simpson, J. H. (1981) The shelf-sea fronts: implications of their existence and behaviour. *Philosophical Transactions of the Royal Society of London* **A302**, 531 - 546.

Simpson, J. H. and R. D. Pingree (1978) Shallow sea fronts produced by tidal stirring. In: M. J. Bowman and W. E. Esaias (editors): *Oceanic fronts in coastal processes.* Springer, Berlin, 29 - 42.

Vachon, P.W., Raney,R.K., Krogstad, H.E., and Liu, A.K., (1993). Airborne synthetic aperture radar observations and simulations for waves-in-Ice. J. Geophysical Research, 98:16,411-16,425.

Vachon, P.W., Krogstad, H.E., and Paterson,J.S., (1994). Airborne and spaceborne synthetic aperture radar observations of ocean waves. Atmosphere-Ocean. 32(10): 83-112.

Vachon P.W., Liu, A. K. and Jackson, F.C. (1995). Near-shore wave evolution observed by airborne SAR during SWADE. Atmosphere-Ocean, 2: 363-381.

Vachon, P.W. and Campbell, J.W.M. and Dobson, F.W., (1997). Comparison of ERS and RADARSAT SARS for wind and wave measurement. Paper Presented at third ERS Symp., ESA, held at Florence, Italy from Mar. 18-2, 1997.

Vogelzang, J., Wensink, G.J., Calkoen, C.J. and van der Kooij, M.W.A. (1997)., Mapping submarine sand waves with multiband imaging radar, 2, Experimental results and model comparison, *J. Geophys. Res.*, **102**, 1183-1192